Simulation of Burnout Processes by a Multi-order Adaptive Network Model

Louis Weyland[1], Wiebe Jelsma[1], and Jan Treur[2](✉)

[1] Computational Science, University of Amsterdam, Amsterdam, The Netherlands
{l.f.weyland,w.a.jelsma}@student.vu.nl
[2] Social AI Group, Vrije Universiteit Amsterdam, Amsterdam, The Netherlands
j.treur@vu.nl

Abstract. In this paper, an adaptive network model for the development of and recovery from burnout was designed and analysed. The current literature lacks adequate adaptive models to describe the processes involved in burnout. In this research, the informal conceptual models from Golembiewski and Leiter-Maslach were combined with additional first- and second-order adaptive components and used to design a computational network model based on them. Four different scenarios were simulated and compared, where the importance of the therapy and the ability to learn from it was emphasised. The results show that if there was no therapy present, the emotion regulation was too poor to have effect. However, at the moment therapy was applied, the emotion regulation would start to help against a burnout. Another finding was that one long therapy session has more effect than several shorter sessions. Lastly, therapy only had a significant long-lasting effect when adaquate neuro-plasticity occurred.

Keywords: Burnout · Second-order adaptive · Network model

1 Introduction

Burnout is defined as a syndrome which occurs after being exposed for a longer time to chronic stress and frustration. The symptoms are mental (emotional) exhaustion, lack of personal accomplishment and depersonalization. Emotional exhaustion corresponds to persisting fatigue with which the person has to deal in his/her daily life. The lack of personal accomplishment represents the depletion of one's productivity. It is linked with being overwhelmed with the slightest task/stress which in turn will impact the effectiveness of efforts made. The depersonalization process characterises the detachment of oneself to his/her work and ambition [9]. Once the burnout stage is reached, the consequence is a psychological trauma which often complicates the integration back into the working-based society.

Given its complex dynamics based on a number of interacting factors, a thorough understanding of the syndrome and its underlying nature is challenging and important. This in return can offer effective intervention and avoid psychological trauma. However,

M. Paszynski et al. (Eds.): ICCS 2021, LNCS 12744, pp. 514–527, 2021.
https://doi.org/10.1007/978-3-030-77967-2_43

not all models provide a consistent and straight forward intervention method. Furthermore, it has been noticed that the current literature is lacking adequate adaptive network models for burnout. In this paper, the revised informal conceptual Leiter-Maslach model is used as inspiration but extended by introducing second-order adaptive network components. It is shown that the adaptive attributes have a non-negligible impact on the simulation of the development of burnout. Furthermore, the adaptive components will play a crucial role in recovery by an effective therapy against burnout.

2 Background Theory

The aforementioned symptoms (exhaustion, lack of personal accomplishment and depersonalization) correspond to the sub-scales of the Maslach Burnout Inventory (MBI) [6]. Many studies base their research on the MBI instrument. However, the order in which the symptoms occur is subject to variation. In literature, well-studied models vary on the order of personal development. In the informal Golembiewski model [1], burnout is described in eight progressive phases which represent a between-subject phase model, starting with depersonalization which impacts the personal accomplishment and leads to emotional exhaustion [1]. According to the model, personal trauma or chronic stress at work could trigger the depersonalization process as a defence mechanism. This leads to low personal accomplishment. Eventually, the emotional exhaustion stage is reached and a full-blown burnout is diagnosed [9]. Another well-known informal model is the Leiter-Maslach model which is a within-subject path model [3].

In the latter model, the process of burnout starts with the emotional exhaustion stage due to the influence of the workload. Then, the repercussion of the emotional exhaustion is the depersonalization phase as a defence strategy (Fig. 1).

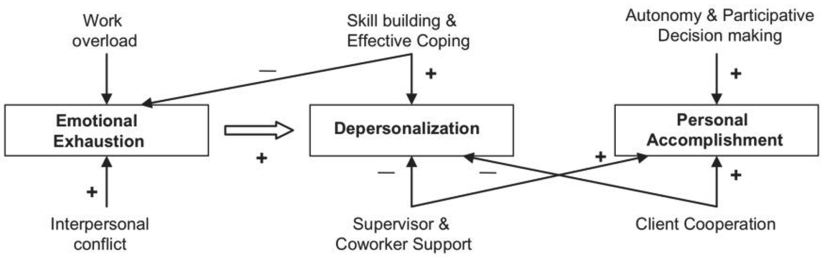

Fig. 1. Leiter-Maslach's informal model [9].

However, in the revised model, the personal accomplishment evolves independent and in parallel to the two MBI factors. Thereby, the three main MBI components are all influenced by external factors such as workload, moral support or internal conflict. In the Golembiewski model, the order of the progressive phases is subject to individual cases, which makes it diffcult to formulate a concrete intervention method. On the other hand, the Leiter-Maslach model formulates that the development of burnout can be prevented if the factors affecting directly the emotional exhaustion are being handled appropriately

[7]. These factors are foremost the workload and personal conflicts. However, it is also mentioned that in advanced stages of a burnout it is advised to undertake organisational changes such as increasing external moral and work support or allowing more autonomy.

As a mental condition, burnout is part of the cognitive neuroscience domain. Hence, it has been shown in the literature that many processes including adaptive behaviour, are reflecting a more accurate image of the studied process [11]. Existing studies proposed an adaptive model for the Maslach model or the job demands-resources model [5, 12]. However, no relevant study has been published on an adaptive Leiter-Maslach model. Additionally, no research has been found to introduce a multi-order adaptive mechanism.

3 The Designed Adaptive Computational Network Model

The designed adaptive network model is based on the revised informal Leiter-Maslach model as shown in Fig. 1. However, a few nodes and connections have been added to the network model (see Fig. 2). First of all, the node Personal accomplishment (which actually concerns lack thereof) has been renamed to Personal non-achievement to better fit its actual meaning and avoid any ambiguity. A connection between depersonalization and personal non-achievement has been created as it is originally in the Maslach model [6]. We believe that a detachment of one's personality affects personal ambitions and objectives. Additionally, a connection between personal non-achievement and workload has been made. An increasing lack of accomplishments will provoke an accumulation of the workload on the other end. An emotion regulation component has been added to the emotional exhaustion. It is known that, based on activity of certain parts of the prefrontal cortex in the brain, a person may control his/her emotional responses and feelings. However, for some people this mechanism may function poorly so that the effect is not sufficient to handle the regulation well.

Furthermore, therapy is added which focuses on improving the emotion regulation explicitly. In the proposed model, for three nodes adaptive characteristics have been included in the network model: the workload, the depersonalization and the emotion regulation. The workload is influenced by personal non-achievement due to which it changes in a non-linear way. The higher the unfulfillment, the more overwhelmed the person will be. Thus the productivity will decrease in a non-linear way. Consequently, the workload will increase in a dynamical fashion. Emotional exhaustion has also underlying adaptive behaviour. Burnout is a slow process, thus the emotion regulation can be seen as an adaptive component where neural networks reorganise based on previous experiences with external stress factors. For the same reasons, the depersonalization has also been equipped with adaptive characteristics.

To represent the network model with its adaptive characteristics well, a multi-order reified temporal-causal network (also called *self-modeling network*) was designed. For its numerical representation, the model was specified by the following *network characteristics*:

- **Nodes** Y (also called states) with state value $Y(t)$ at each time point t.
- **Connectivity** defined by connections from node X to Y and described by their *connection weight* $\boldsymbol{\omega}_{X,Y}$.

- **Aggregation** defined by *combination functions* $\mathbf{c}_Y$ determining how multiple incoming single impacts $\boldsymbol{\omega}_{X,Y}Y(t)$ on one node Y are aggregated.
- **Timing** defined by *speed factors* $\boldsymbol{\eta}_Y$ specifying how fast the state of a node Y changes based on the incoming aggregated impact.

Based on the above network characteristics, the underlying standard difference equation used for all nodes Y is

$$Y(t + \Delta t) = Y(t) + \boldsymbol{\eta}_Y[\mathbf{c}_Y(\boldsymbol{\omega}_{X_1,Y}X_1(t), \ldots, \boldsymbol{\omega}_{X_k,Y}X_k(t)) - Y(t)]\Delta t \quad (1)$$

where X_1, …, X_k are the nodes from which Y gets incoming connections. Note that when modeling a specific person and/or context, these network characteristcs are used to represent personal and/or contextual characteristics, including individual differences. In this way such a network model can be used for a wide variety of specific circumstances.

Equations (1) are already given in the available dedicated software environment; see [10], Ch 9. Within the software environment described there, around 40 useful basic combination functions are included in a combination function library; see Table 1 for the ones used in this paper. The selected ones for a model are assigned to states Y by specifying combination function weights $\boldsymbol{\gamma}_{i,Y}$ and their parameters used by $\boldsymbol{\pi}_{i,j,Y}$.

Note that 'network characteristics' and 'network states' are two distinct concepts for a network. Self-modeling (or reification) is a way to relate these distinct concepts to each other in an interesting and useful way:

- A *self-model* is making the implicit network characteristics (such as connection weights $\boldsymbol{\omega}$ or excitability thresholds $\boldsymbol{\tau}$) explicit by adding states for these characteristics; thus the network gets a self-model of part of the network structure; this can easily be used to obtain an *adaptive network*.
- In this way, multiple self-modeling levels can be created where network characteristics from one level relate to states at a next level. This can cover *second-order* or *higher-order adaptive networks*; see, for example, [10, 11].

Adding a self-model for a given temporal-causal (base) network is done in the way that for some of the states Y of this base network and some of its related network structure characteristics for connectivity, aggregation and timing (in particular, some from $\boldsymbol{\omega}_{X,Y}$, $\boldsymbol{\gamma}_{i,Y}$, $\boldsymbol{\pi}_{i,j,Y}$, $\boldsymbol{\eta}_Y$), additional network states $\mathbf{W}_{X,Y}$, $\mathbf{C}_{i,Y}$, $\mathbf{P}_{i,j,Y}$, $\mathbf{H}_Y$ (*self-model states*) are introduced:

a) **Connectivity self-model**
Self-model states $\mathbf{W}_{Xi,Y}$ are added representing connectivity characteristics, in particular connection weights $\boldsymbol{\omega}_{Xi,Y}$

b) **Aggregation self-model**
Self-model states $\mathbf{C}_{j,Y}$ are added representing aggregation characteristics, in particular combination function weights $\boldsymbol{\gamma}_{i,Y}$
Self-model states $\mathbf{P}_{i,j,Y}$ are added representing aggregation characteristics, in particular combination function parameters $\boldsymbol{\pi}_{i,j,Y}$

c) **Timing self-model**
   Self-model states $\mathbf{H}_Y$ are added representing timing characteristics, in particular speed factors $\boldsymbol{\eta}_Y$

The notations $\mathbf{W}_{X,Y}$, $\mathbf{C}_{i,Y}$, $\mathbf{P}_{i,j,Y}$, $\mathbf{H}_Y$ for the self-model states indicate the referencing relation with respect to the characteristics $\boldsymbol{\omega}_{X,Y}$, $\boldsymbol{\gamma}_{i,Y}$, $\boldsymbol{\pi}_{i,j,Y}$, $\boldsymbol{\eta}_Y$: here $\mathbf{W}$ refers to $\boldsymbol{\omega}$, $\mathbf{C}$ refers to $\boldsymbol{\gamma}$, $\mathbf{P}$ refers to $\boldsymbol{\pi}$, and $\mathbf{H}$ refers to $\boldsymbol{\eta}$, respectively. For the processing, these self-model states define the dynamics of state Y in a canonical manner according to Eqs. (1) whereby $\boldsymbol{\omega}_{X,Y}$, $\boldsymbol{\gamma}_{i,Y}$, $\boldsymbol{\pi}_{i,j,Y}$, $\boldsymbol{\eta}_Y$ are replaced by the state values of $\mathbf{W}_{X,Y}$, $\mathbf{C}_{i,Y}$, $\mathbf{P}_{i,j,Y}$, $\mathbf{H}_Y$ at time t, respectively. As the outcome of the addition of a self-model is also a temporal-causal network model itself, as has been shown in detail in [10], Ch 10, this construction can easily be applied iteratively to obtain multiple levels of self-models.

For the designed model, four different combination functions were used; see Table 1. For nodes with one incoming connection, the identity function was used. For nodes with multiple incoming connections, the advanced logistic sum combination function was used see the second row in the table. Table 2 provides an overview of all nodes of the network model; note that when using these functions in (1), the variables V, V_i are applied to single impacts $\boldsymbol{\omega}_{X,Y}Y(t)$.

Table 1. Basic combination functions from the library used in the presented model

	Notation	Formula	Parameters
Identity	$\mathbf{id}(V)$	V	-
Advanced logistic sum	$\mathbf{alogistic}_{\sigma,\tau}(V_1, \ldots, V_k)$	$[\frac{1}{1+e^{-\sigma(V_1+\cdots+V_k-\tau)}} - \frac{1}{1+e^{\sigma\tau}}](1+e^{-\sigma\tau})$	Steepness $\sigma > 0$ Threshold τ
Hebbian learning	$\mathbf{hebb}_{\mu}(V_1, V_2, W)$	$V_1V_2(1-W)+\mu W$	Persistence factor $\mu > 0$
Stepmod	$\mathbf{stepmod}_{\rho,\delta}(V_1, \ldots, V_k)$	0 if t mod $\rho < \delta$, else 1	Repetition ρ Duration δ

The first-order self-model states are: Workoverload adaptation, Depersonalisation adaptation and Emotion regulation adaptation. In terms of the above explanation and terminology, these three states are $\mathbf{W}$-states representing weights $\boldsymbol{\omega}$ of connections between base states: respectively, from state Personal nonachievement to Workoverload, and from state Emotional exhaustion both to Depersonalisation and Emotion regulation control. The adaptation mechanisms for them were based on Hebbian learning. In the literature, Hebbian learning has shown adequate results [2]. It reinforces connections of nodes that are activated simultaneously:

'Neurons that fire together, wire together'

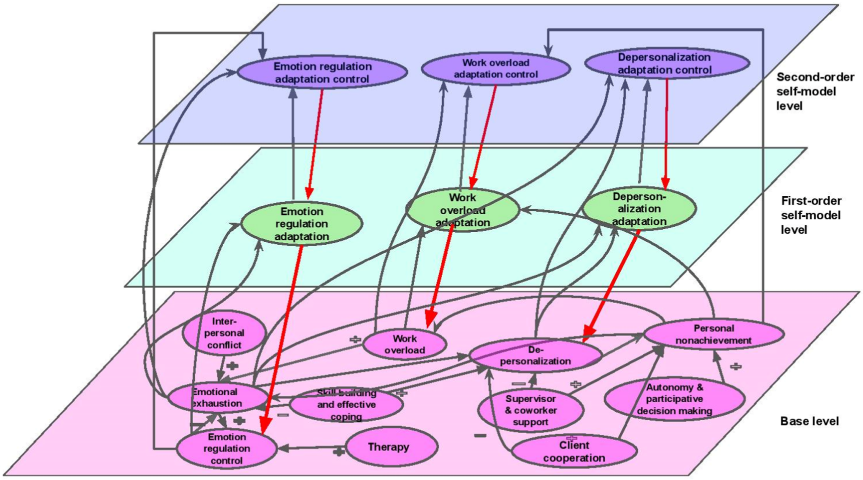

Fig. 2. Extended Leiter-Maslach model by introduction of first- and second-order adaptation. Furthermore, a direct connection from depersonalization to personal non-achievements is made. Finally, an emotion regulation and therapy component is added. The red connections represent the effects of the self-models on the adaptive network characteristics. (Color figure online)

The formula shown in the third row of Table 1 models this Hebbian learning principle where W corresponds to the value of the first-order connection weight self-model **W**-state and V_1,V_2 represent the activation levels *X(t)* and *Y(t)* of the connected base states X and Y. The second-order adaptation nodes are Workoverload adaptation control, Depersonalisation adaptation control, and Emotion regulation adaptation control. Given the above explanation and terminology, these three states are **H**-states representing the speed factors $\boldsymbol{\eta}$ of the related first-order **W**-states. They control the three types of adaptation modeled by the first-order self model **W**-states. For the second-order self-model states, the advanced logistic sum combination function was used for the aggregation [11]. These second-order nodes model that the speed factors $\boldsymbol{\eta}$ of the related first-order nodes are adaptive. Through this, the learning process was equipped with an adaptive learning rate which changes over time depending on influences of the external factors. The second-order adaptation (also called *metaplasticity*) principle modeled here is:

'Adaptation accelerates with increasing stimulus exposure' ([8], p. 2).

The fourth combination function was used specifically for the therapy node and is referred as steppmod function. It creates a repeated occurrence of an external factor (here the therapy) with some time duration and time of resting.

The model was implemented using the available dedicated software environment in Matlab, using a library for combination functions; see [10], Ch 9. The role matrices fully specifying the adaptive network model are shown in the Appendix [13].

Table 2. Overview of the states in the network model

State	Name	Level
X_1	Workoverload	Base level
X_2	Interpersonal conflict	
X_3	Skill building and effective coping	
X_4	Supervisor and coworker support	
X_5	Autonomy and participative decision	
X_6	Client cooperation	
X_7	Emotional exhaustion	
X_8	Depersonalisation	
X_9	Personal nonachievement	
X_{12}	Emotion regulation control	
X_{10}	Workoverload adaptation	First-order self-model
X_{11}	Depersonalisation adaptation	
X_{13}	Emotion regulation adaptation	
X_{14}	Workoverload adaptation control	Second-order self-model
X_{15}	Depersonalisation adaptation control	
X_{16}	Emotion regulation adaptation control	
X_{17}	Therapy	Base level

4 Simulation Results

Four different scenarios were simulated. The first scenario shows the simulation of developing a burnout, without therapy. The second scenario simulates a developed burnout with short and frequent therapy sessions. The third one simulates a burnout with longer and less frequent therapy sessions. The fourth scenario shows a therapy session where the higher-order adaptation of emotion regulation is deactivated.

For each scenario, a fictive character with a tendency to develop a burnout was addressed. This was achieved by setting a higher interpersonal conflict and low support from the external factors, such as the Client cooperation or Supervisor/Co-worker support. According to the complex causal relationships as modeled, the external factors influence the development. To trigger a burnout, for the first three scenarios, a high workload was set. The initial value for the connection weight representation for emotion regulation was set to a very low value, thus representing a person with very poor emotion regulation capabilities: 0.0005. The external factors are set to relatively low values. The connections from the first-order states to the second-orders were set to −0.2 to avoid an exaggerated learning rate. Additionally, the speed factor for the workload was decreasing. The base nodes emotional exhaustion, depersonalization and personal non-achievement were all set to a low initial value of 0.03 to represent a very healthy starting point for the person. The second-order speed factors were set to 0.001. Concerning the advanced logistic sum combination function, the threshold for the depersonalization and the second-order depersonalization was set slightly higher than for the emotional exhaustion and personal non-achievement due to a higher number of incoming connections. By doing so, the excitation of the node is delayed and an early triggering is circumvented. For the Hebbian function, the persistence factor μ was set to 0.98 for all first-order adaptation nodes. Therefore the learning is effective, most what is learned will be remembered (only 2% loss per time unit). The simulation was set to a duration of 20000 time units (but the graphs shown in Figs. 3 and 7 only display a focus on a shorter time interval). The step size Δt was set to 0.5. The external factors are not shown in the figures due to the fact that they are constant and don't significantly contribute to the understanding of the figures.

Scenario 1: Development and Persistence of Burnout Without Therapy

Figure 3 shows the simulation with an initial high workload and no therapy. One can see a rapid increase in the emotional exhaustion. For the depersonalization and personal non-achievement, a short dip is noticeable before they increases rapidly and go to an equilibrium. The dip is caused by the second-order dip at the beginning.

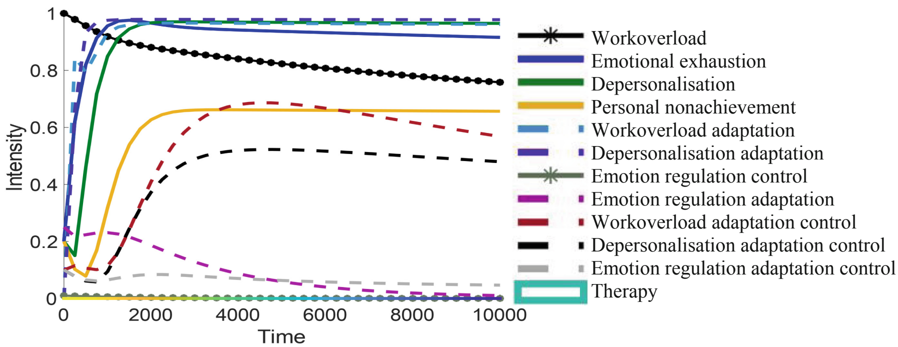

Fig. 3. Running the simulation with a duration of 10000 and a step size Δt of 0.5. The simulation starts with a high workload, no therapy is applied.

The emotion regulation and corresponding adaptive nodes stay largely unaffected in this simulation. The therapy here shown by the rainbow coloured line is set to 0.

Scenario 2: Short Therapy Sessions

Figure 4 (upper graph) shows the simulation with short and repetitive therapy sessions. As expected, the simulation has the same initial evolution as in Scenario 1. However, due to influences of the therapy a more complex pattern emerges. The therapy starts at $t = 3000$ and repeats itself in short intervals of 1500 time units. First of all, a constant decrease of the workload can be observed. Emotional exhaustion, depersonalization and personal non-achievement fluctuate in a periodic manner. During the therapy, the three Maslach sub-scales decrease. In between, the sub-scales underwent a small increase. However, in overall, the sub-scales decreased. All the first-order nodes increase immediately and stay around an equilibrium.

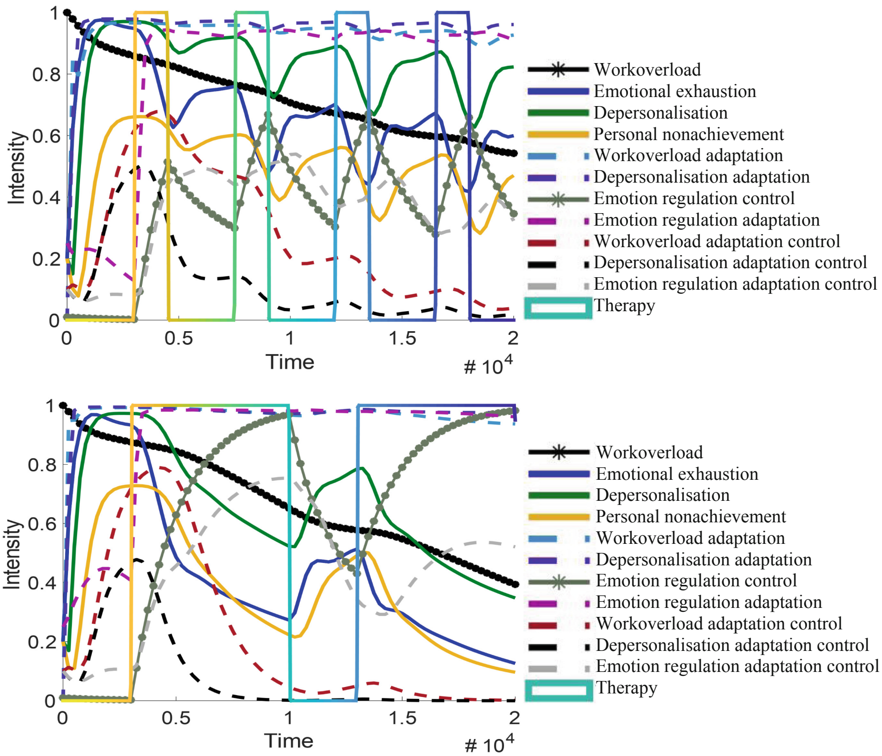

Fig. 4. Running the simulation with a duration of 20000 time units and a step size Δt of 0.5. The upper graph (Scenario 2) starts with high workload, while over time short and frequent therapy sessions are applied. The lower graph (Scenario 3) starts with high workload, while over time long therapy sessions are applied.

Once the therapy was activated, an instantaneous increase of the first-order adaptation states for emotional regulation and the emotional regulation itself were provoked. However, between the sessions, the emotion regulation decreased. The second-order adaptation of emotion regulation had a steady fluctuation before the therapy. During the therapy and shortly after, the second-order adaptation states increased. In the middle of the in-between sessions, the second-order adaptation states seemed to decrease. The second-order adaptation states for workload and for depersonalization nodes underwent a decrease after the first therapy.

Scenario 3: Long Therapy Sessions

Scenario 3 (Fig. 4 lower graph) used the same parameters as in Scenario 2. However, the duration of the therapy was set to a duration of 7000 time units. Before the therapy, the same pattern as described before can be observed. During the therapy, an important increase of the emotion regulation is noticeable. Furthermore, a significant decrease of the emotional exhaustion, depersonalization and personal non-achievement can be seen during the therapy. At $t = 10000$, the three sub-scales had a lower value compared to the simulation in Scenario 2. The second-order adaptation state for emotion regulation has reached overall higher values.

Scenario 4: Short Therapy and No Second-Order Neuro-Plasticity

Scenario 4 (see Fig. 5) was build upon Scenario 3. However, the emotion regulation was not made adaptive. Thus, one can see that the second-order adaptation state for emotion regulation is not active (constant) during the simulation. The first-order adaptation state for emotion regulation starts to increase once the first therapy starts but doesn't increase further after the consecutive therapies. A fast-growing trend can be observed for the Maslach sub-scales. During the therapy sessions, the emotional exhaustion, depersonalization and the personal non-achievement decrease slowly. In the end, these nodes seem to undergo periodical fluctuations.

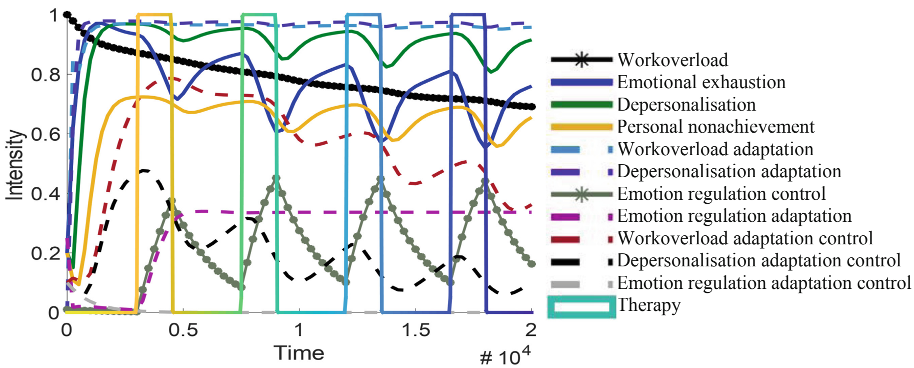

Fig. 5. A simulation (Scenario 4) with a duration of 20000 time units and a step size Δt of 0.5. The simulation is run with short therapies and no adaptive behaviour for the emotional regulation.

5 Verification by Mathematical Analysis of Stationary Points

In scientific computing, truncating error and rounding error induce inaccurate results. Additionally, the time steps Δt used for the integration can produce unstable algorithms with important deviation to the true results. Therefore, it is important to verify the exactness of the implemented model. The verification of the model can be done by comparing the theoretically determined values based on the high-level specification of the model to the ones computed in a simulation generated by the implemented model.

This verification was done by selecting randomly points at times t where a considered node Y of the model is stationary, i.e., $dY(t)/dt = 0$. According to difference Eq. (1), if $\boldsymbol{\eta}_Y > 0$, being stationary is equivalent to the standard criterion

$$\mathbf{c}_Y(\boldsymbol{\omega}_{X_1,Y}X_1(t), \ldots, \boldsymbol{\omega}_{X_k,Y}X_k(t)) = Y(t) \tag{2}$$

where $X_1, \ldots, X_k$ are the nodes from which Y gets incoming connections. Here, the left hand side is also denoted by $\mathbf{aggimpact}_Y(t)$; this is what we call here theoretical value, whereas for the state value at the right hand side the simulation value is used. Thus, the deviation between the theoretical and simulation value indicates the accuracy of the model. In this case, the verification was applied to the model in Scenario 1. From each level, a random node was selected for the analysis. Thus for the picked nodes Y the theoretical values computed by the formula from Table 1 were compared to the value $Y(t)$ from the simulation. The deviations found are small (see Table 3), which provides evidence that the implemented model is correct with respect to the high-level model specification.

Table 3. Verification results.

State X_i	Personal non-achievement	First-order adaptation for workload	Second-order adaptation for emotion regulation
Time point t	200000	200000	200000
$X_i(t)$	0.9584	0.9638	0.0350
$\mathbf{aggimpact}_{X_i(t)}$	0.9432	0.9712	0.0354
Deviation	0.0152	0.0074	0.0004

6 Model Validation

The challenge in burnout research is the quantification of the different stages. In [4], empirical data was collected using a latent profile analysis with 5-class scale (see Fig. 6). Each stage is characterised by the combination of the different scores for exhaustion, cynicism (depersonalization) and efficiency. For the fine-tuning, the scale was normalised to a maximum of 1 instead of 5. Thus, by doing so, the score can be expressed in percentage where 100% means a score of 1 out of 1.

The burnout stage as it is described in [4] would have a score of 100% for exhaustion, 84% for cynicism and 60% (see the empirical values in Table 4). For the validation, the two stages burnout and ineffective were chosen.

An ineffective profile means that the personal non-achievement is high without compromising the mental health of a person. The simulation without therapy was chosen to be fine-tuned. The validation process entailed time-consuming computations. Thus the maximum time t was set to 5000 and the step size Δt to 0.5. Furthermore, the number of parameters fine-tuned was limited to 3. From these, one corresponded to the initial value of emotional exhaustion. The other two parameters fine-tuned were the speed factors of the depersonalization and personal non-achievement. The empirical data to which the model was fine-tuned were chosen to arbitrarily with the end value corresponding to the empirical values found in [4]. The parameter tuning was done using a simulated annealing algorithm from Matlab's Optimization Tool. The root means square error (RMSE) was chosen as an error function. The results are shown in Table 4. An example simulation after the fine-tuning in comparison to the data points used is shown in Fig. 7.

Class	**N**	**Exhaustion**	**Cynicism**	**Inefficacy**
Burnout	48 (4%)	5.04	4.19	2.98
Disengaged	136 (12%)	4.67	3.78	1.22
Overextended	201 (17%)	4.18	1.62	0.92
Ineffective	235 (20%)	2.54	1.99	2.43
Engagement	546 (47%)	1.81	0.87	0.82
Overall	1166	2.83	1.70	1.30
SD		1.46	1.30	0.92

Fig. 6. Visualisation (left) of 5 different progressive stages included the final burnout stage with their respective score determined in [4]. The table (right) contains the score of the Maslach Subscales for the different stages. The column N corresponds to the percentages of patients diagnosed with the respective stage.

Table 4. Results from fine-tuning the model to the different stages from [4] using Matlab's Optimization Tool

		Emotional exhaustion		Depersonalization		Personal non-achievement	
	RMSE	Empirical values	Computed values	Empirical values	Computed values	Empirical values	Computed values
Burnout	0.17	100%	91%	84%	94%	60%	70%
Ineffective	0.35	50%	40%	40%	30%	49%	21%

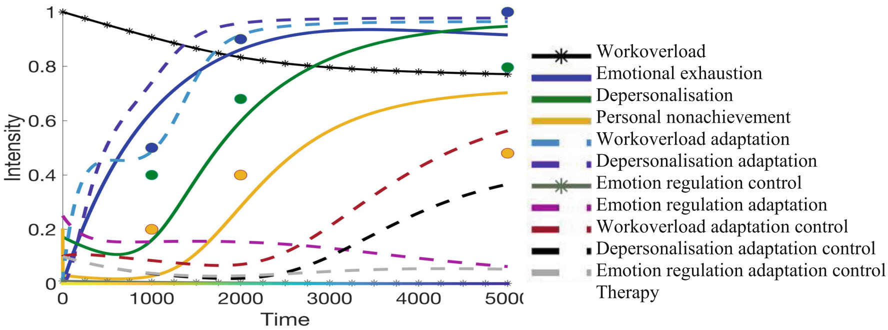

Fig. 7. Fine-tuning result for the model to the burnout stage determined in [4]. The numerical results are shown in Table 4.

7 Discussion and Conclusion

The simulations have shown promising results. In accordance with the literature, a burnout is triggered by having high emotional exhaustion, depersonalization and personal non-achievement (Fig. 4). However, the interesting results are shown in Fig. 5 where the importance of the first and second-order components of the model are shown. Especially, the impact on the emotion regulation is of great interest. Before the therapy, when the symptoms increased rapidly, the ability to cope with the situation were poor. The emotion regulation had no impact on the situation. Furthermore, the learning rate was constant. However, once the therapy started, an instant increase in the emotion regulation emerged. The learning capacity improved fast due to an adaptive learning rate that became higher. Despite a small decrease of the emotion regulation between the therapy sessions, the learning ability is retained over time, which allows to further increase the emotion regulation for each therapy. Comparing to Fig. 5 (lower), one can see that one longer therapy shows to be more effective than having multiple shorter sessions. The speed of learning how to regulate the emotions increased further.

In Scenario 4, a simulation was conducted where no second-order neuro-plasticity occurs. In this case, the previous experiences and therapy have no long-term effect since the ability to learn from it is limited. Thus, one can see that after each therapy, the emotion regulation regress to earlier stages. The second-order adaptation state for emotion regulation node had no effect over the whole simulation. The first-order adaptation state increases only after the first therapy. In other words, after the first therapy, the first-order adaptation state was not further stimulated. Thus the results show that without second-order plasticity, the therapy has limited effect. Since we know that in practice the therapy is effective and essential, second-order neuro-plasticity must occur. Thus, (second-order) adaptive behaviour and adaptive learning from previous experiences play an important role and need to be taken into account.

In [5] also an adaptive network model was shown for burnout. A main difference compared to the current model is that in [5] no second-order adaptation is modelled. A similar difference applies to [12]. Another difference with [5] is that their focus is on the role of dreaming whereas for the current model it is on the informal models from [1] and [4], which were not considered in [5].

The study could be taken further were the environmental nodes such as personal conflict, client cooperation, skill-building and such vary over time. By creating a feedback loop from the Maslach sub-scales to the environmental nodes, a more refined model can be created.

References

1. Golembiewski, R.T., Munzenrider, R., Carter, D.: Phases of progressive burnout and their work site covariants: critical issues in OD research and praxis. J. Appl. Behav. Sci. **19**(4), 461–481 (1983)
2. Hebb, D.O.: The Organization of Behavior: A Neuropsychological Theory. Chapman & Hall, London (1949)
3. Leiter, M.P.: Burnout as a developmental process: consideration of models. In: Schaufeli, W., Maslach, S., Marek, T. (eds.) Professional burnout: Recent developments in theory and research, pp. 237–250. Taylor and Francis, Washington (1993)
4. Leiter, M.P., Maslach, C.: Latent burnout pro les: a new approach to understanding the burnout experience. Burn. Res. **3**(4), 89–100 (2016)
5. Maijer, M., Solak, E., Treur, J.: An adaptive network model for burnout and dreaming. In: Krzhizhanovskaya, V.V., et al. (eds.) ICCS 2020. LNCS, vol. 12137, pp. 342–356. Springer, Cham (2020). https://doi.org/10.1007/978-3-030-50371-0_25
6. Maslach, C., Jackson, S.E., Leiter, M.P.: The Maslach Burnout Inventory. Consulting Psychologists Press, Palo Alto (1981)
7. Richardsen, A.M., Burke, R.J.: Models of burnout: Implications for interventions. Int. J. Stress Manag. **2**(1), 31–43 (1995)
8. Robinson, B.L., Harper, N.S., McAlpine, D.: Meta-adaptation in the auditory midbrain under cortical influence. Nat. Commun. **7**, e13442 (2016)
9. Sharma, R.R., Cooper, C.L.: Executive Burnout: Eastern and Western Concepts, Models and Approaches for Mitigation. Emerald Group Publishing, Bradford (2016)
10. Treur, J.: Network-Oriented Modeling for Adaptive Networks: Designing Higher-Order Adaptive Biological, Mental and Social Network Models. Springer, Cham (2020). https://doi.org/10.1007/978-3-030-31445-3
11. Treur, J.: Network-Oriented Modeling: Addressing Complexity of Cognitive, Affective and Social Interactions. Springer, Cham (2016). https://doi.org/10.1007/978-3-319-45213-5
12. Veldhuis, G., Sluijs, T., van Zwieten, M., Bouwman, J., Wiezer, N., Wortelboer, H.: A proof-of-concept system dynamics simulation model of the development of burnout and recovery using retrospective case data. Int. J. Environ. Res. Public Health **17**(16), 5964 (2020). https://doi.org/10.3390/ijerph17165964
13. Appendix (2021). https://www.researchgate.net/publication/348405068